Effect of Postmortem Time and Preservation Fluid on the Tensile Material Properties of Bovine Liver Parenchyma

K. M. Dunford[1] and A.R. Kemper[1]
[1] Center for Injury Biomechanics, Virginia Tech - Wake Forest University

ABSTRACT

The liver is one of the most frequently injured abdominal organs in motor vehicle collisions (MVCs). However, currently accepted anthropomorphic test devices are unable to predict abdominal organ injury risk. Consequently, finite element models are becoming an important tool for assessing abdominal organ injury risk in MVCs. However, in order to accurately assess injury risk, these models must be validated based on biomechanical data. Previous studies have quantified the tensile failure properties of human liver parenchyma, but have been limited to testing at 48hrs postmortem. Although a previous study found no significant changes in the tensile failure stress or strain of bovine liver between 6 and 48 hours postmortem when the tissue was stored in DMEM, the effects of postmortem degradation may vary with respect to the type of preservation fluid used. Therefore, the purpose of this study was to quantify the effects of postmortem degradation on the tensile material properties of bovine liver parenchyma with increasing postmortem time when stored in saline and then compare the effects of saline versus DMEM on material property degradation. Uniaxial tension tests were conducted on parenchyma samples of five bovine livers acquired immediately after death. Tissue was immersed in normal saline and kept cool (i.e., never frozen) during preparation and storage. Multiple dog-bone samples from each liver were tested once to failure at three time points: ~6hrs, 24hrs, and 48hrs after death. The data were then analyzed using a Block ANOVA to determine if there were significant changes in the failure stress and failure strain with respect to postmortem time. The average failure stresses were 50.4±12.9kPa, 55.3±15.6kPa, and 54.7±22.0kPa at the 6hr, 24hr, and 48hr time points, respectively. The average failure strains were 0.28±0.023, 0.25±0.025, and 0.24±0.013, at the 6hr, 24hr, and 48hr time points, respectively. The results of the current study show that the failure strain of bovine liver parenchyma decreases significantly between 6hrs and 48hrs after death when stored in saline and refrigerated. Conversely, neither the failure stress nor failure strain changed significantly with respect to postmortem time when stored in DMEM. Overall, this study illustrates that the effects of postmortem liver degradation varies with respect to the preservation fluid. Specifically, DMEM was found to preserve the material properties of liver parenchyma more effectively than saline within the first 48hrs postmortem.

INTRODUCTION

The liver is one of the most commonly injured abdominal organs in motor vehicle related trauma (Duckworth, 2008). Its susceptibility to injury in blunt trauma is due to its size, location, fixed position, and abundant vasculature (Malaki, 2011). Anthropomorphic testing devices (ATDs) are currently used to evaluate injury risk in motor vehicle collisions (MVCs) using biomechanically based risk functions. However, currently accepted ATDs are not equipped to represent internal abdominal organs (Klinich, 2010). Therefore, researchers frequently rely on finite element models (FEMs) to assess abdominal organ injury risk in MVCs. In order for FEMs to accurately predict the risk of injury to individual organs, they must be validated based on biomechanical data. There have been several studies that have quantified the failure material properties of human, bovine, and porcine liver tissue by performing tension and compression tests on isolated samples (Uehara, 1995; Stingl, 2002; Santago, 2009a; Santago, 2009b; Kemper, 2010; Kemper, 2013). However, these studies were limited to conducting tests on the tissue at 24 hours or 48 hours postmortem.

The material response of biological tissue can change substantially once removed from living state due to the lack of blood supply, changes in temperature, changes in hydration, differences in boundary conditions, and postmortem degradation (Ottensmeyer, 2001). Some studies have evaluated the effect of postmortem time on liver tissue at a cellular level. Cell swelling was observed in guinea pig livers within two hours postmortem when stored in saline (Popovic, 1989), while cell swelling has been observed in rat livers at just one hour post mortem when *in situ* (Tomita, 2004). The observed degradation within 24 hours of death at a cellular level needs to be quantified in the tissue level response. A previous study by Tay et al, conducted indentation tests on porcine liver tissue at multiple time points up to 48 hours postmortem (Tay, 2006). Tests were completed *in vivo*, *in situ*, and *in vitro*. The *in vitro* tissue was kept cool and stored in saline for 6 to 48 hours postmortem. The results showed an increase in stiffness of the tissue with increased postmortem time. To the author's knowledge, only one study has evaluated the effects of postmortem degradation on the tensile failure properties of liver parenchyma within 24 hours. Dunford et al. conducted uniaxial tension tests on bovine liver parenchyma at 6hrs, 24hrs, and 48hrs postmortem (Dunford, 2017). In this study, the liver tissue was stored as large blocks and submerged in Dulbecco's Modified Eagle Medium (DMEM) between the three time points. The tensile material testing showed that the failure stress and strain did not change significantly with postmortem time. However, this study did not evaluate the effects of preservation fluid on the degradation effects over time. As noted previously, other studies have reported changes in liver tissue at the cellular level and mechanical response when stored in saline. Therefore, the goal of this study is to quantify the effects of postmortem degradation on the failure stress and strain of bovine liver parenchyma in tension when the tissue is preserved in saline.

METHODS

Tissue Tension Testing

Uniaxial tension tests were conducted on samples from five bovine livers. The livers were obtained from a local slaughterhouse immediately after death. During transport to the lab, the livers were sealed in a plastic bag and stored in a cooler on wet ice. The livers were not frozen at any point between procurement and testing since freezing has been shown to affect the material properties (Santago, 2009).

A number of detailed steps were followed to obtain multiple dog-bone samples from each liver at each time point (Kemper, 2010). The first step in obtaining dog-bone samples was to cut a block of tissue from the liver. The rectangular block was then inserted into a custom slicing jig that secured the tissue during slicing (Figure 1). Long blades were drawn across the block in order to create rectangular tissue slices of constant thickness. The rectangular slices were then immersed in saline until stamping. During stamping, the tissue slices were positioned on a base using a template so that defects and visible vasculature would not be included in the dog-bone sample. After removing the template, a custom stamp was placed over the tissue using guide rods and then struck firmly with a hammer to cut the tissue. The resulting dog-bone samples were submerged in saline until testing. The remaining liver tissue that was not used for the 6 hour testing was divided into large sections and placed into containers. The containers were filled with normal saline so that the tissue was completely submerged, sealed, and kept cool until the 24 hour or 48 hour time points. The cutting and stamping procedure was repeated at the remaining two time points.

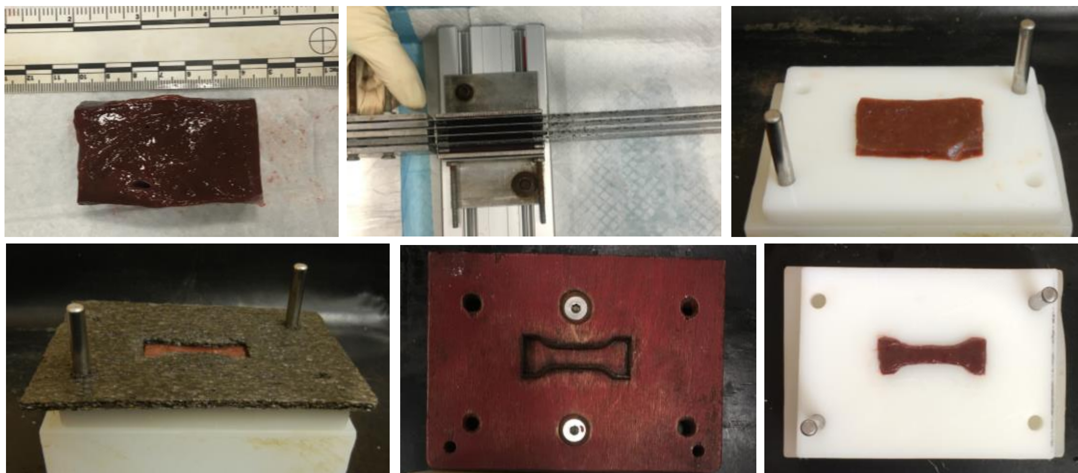

Figure 1: Tissue Block (top left), Slicing Jig and Blade Assembly (top center), Tissue Slice (top right), Template over Slice (bottom left), Custom Stamp (bottom center), and Cut Sample (bottom right).

Uniaxial tension tests were conducted on the dog-bone parenchyma samples at room temperature. The testing procedures were developed to minimize variation in initial specimen slack and alignment (Figure 2) (Kemper, 2010). First, the top grip assembly was placed on a table top. The sample was positioned on the top grip so that the long axis of the specimen aligned with the main axis of the grip and load train. Once aligned, the top portion of the sample was secured to the top grip. White circular paint markers were applied to the surface of the gage region of the specimen. Then, the top grip assembly was reattached to the testing device. The sample was allowed to hang under its own weight (i.e., 1g preload) before being clamped into the bottom grip. This allowed for a proportionally consistent tensile preload. A high resolution digital camera was used to take side view pictures of the mounted sample in order to obtain initial specimen thickness. High-speed video was taken of the front-face of the specimen during each test. The pre-test frames were used to determine initial specimen width. The testing apparatus was operated with a multi-axis controller that simultaneously moved the top and bottom grips at a constant velocity away from each other. Each specimen was loaded to failure at a strain rate of $1s^{-1}$. The high-speed video was recorded at 500 frames/s with a resolution of 10.3 pixels/mm. Load cell, potentiometer, and accelerometer data were sampled at 20,000Hz.

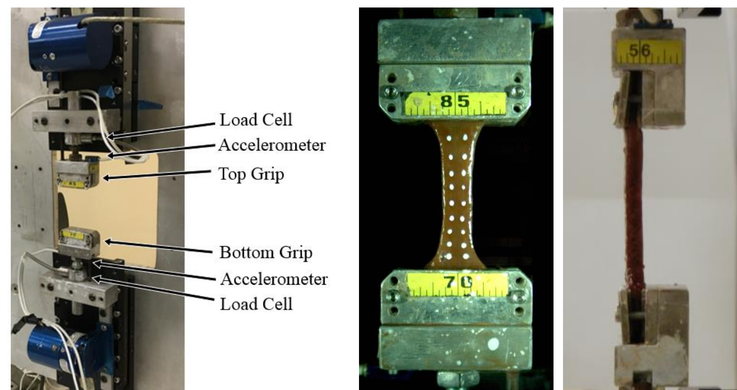

Figure 2: Uniaxial Experimental Setup (left) and Mounted Tissue Specimen (center, right).

Data Processing

The white paint markers on the front face of the sample were tracked using motion analysis software (TEMA, Image Systems, Sweden). The stretch ratio (λ) and Green-Lagrangian strain (E) were calculated using the locations of the markers surrounding the location of failure tear initiation. The instantaneous vertical distance between two dots (L_n) was determined at each video frame, while the original distance between the dots (L_o) was determined from a pre-movement frame. The vertical distance between the two dots was fit using a 6th degree polynomial from the time the grips began moving until the failure tear initiated (Kemper, 2010).

$$E = \frac{1}{2}(\lambda^2 - 1) \quad \text{(Equation 1)}$$

$$\lambda = \frac{L_n}{L_o} \quad \text{(Equation 2)}$$

The grip acceleration (a), effective mass (m_{eff}), and measured force (F) were used to calculate the inertially compensated force (F_{IC}). The inertially compensated force was then fit using a 6th degree polynomial from the time the grips began moving until failure tear initiation. The 2nd Piola Kirchhoff Stress (S) was then calculated at each frame within this time range. The stretch ratio, initial cross-sectional area at the tear location (A_o), and inertially compensated force were used to calculate the stress.

$$F_{IC} = F - a * m_{eff} \quad \text{(Equation 3)}$$

$$S = \frac{F_{IC}}{\lambda * A_o} \quad \text{(Equation 4)}$$

The failure stress and strain were calculated for each sample, then averaged amongst the successful tests at each time point for each liver. The average failure stress and failure strain were compared among the three time points for each liver and between all five livers. A Block ANOVA, where each liver was treated as a block, was used to determine any significant changes in failure values with respect to postmortem time. Significance was defined as $p \leq 0.05$.

RESULTS

For all five livers, there were between two and five successful tests per time point. A total of 117 tests were conducted, resulting in 51 successful tests. Exemplar, stress-strain curves from one liver are shown in Figure 3. The average failure stresses across all five livers were 50.4±12.9kPa, 55.3±15.6kPa, and 54.7±22.0kPa at the 6hr, 24hr, and 48hr time points, respectively. The average failure strains were 0.28±0.023, 0.25±0.025, and 0.24±0.013, at the 6hr, 24hr, and 48hr time points, respectively. Figure 4 compares the average failure stresses and strains from each liver at each time point. Figure 5 compares failure stresses and strains normalized to the Time 0 failure values. The Block ANOVA test showed that there were no significant differences in failure stress with respect to postmortem time. However, the failure strain decreased significantly with increased postmortem time.

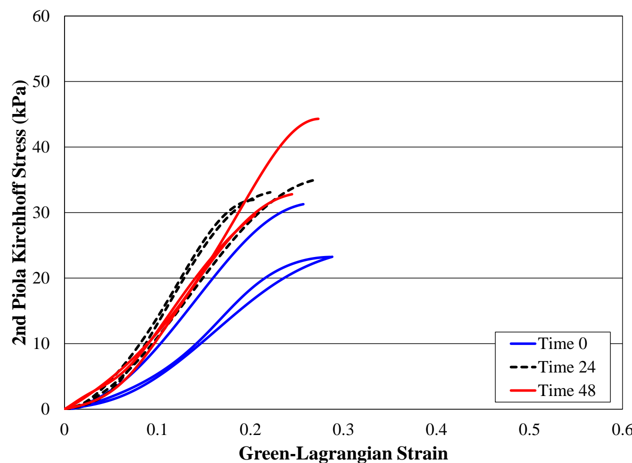

Figure 3: Stress-Strain Curves from One Liver for the Three Time Points.

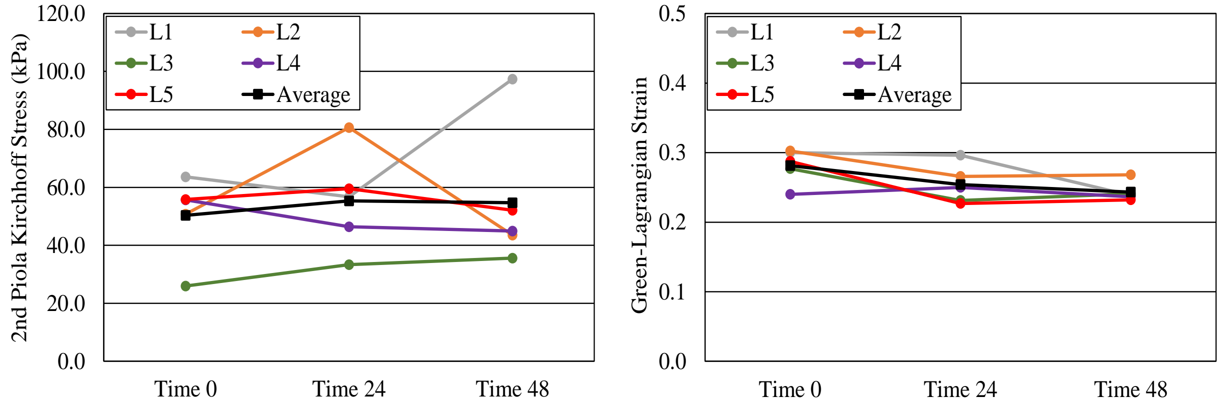

Figure 4. Average Failure Stress (left) and Strain (right) at 6hr, 24hr, and 48hr Time Points.

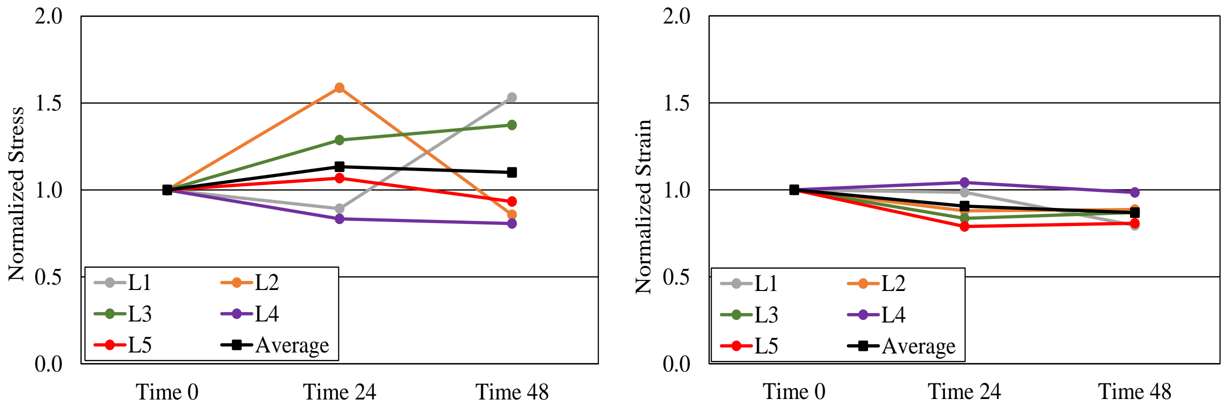

Figure 5. Normalized Average Failure Stress (left) and Strain (right) at each Time Point.

DISCUSSION

In the current study, 51 tension tests were successfully performed on five bovine livers at three time points. The tensile failure stresses and strains from the current study closely align with those from previous studies. Kemper et al. found similar results when testing human liver samples at a strain rate of 1 s^{-1} (Kemper, 2010). This study found an average failure stress of 52.61 ± 25.73kPa and an average failure strain of 0.30 ± 0.10. The previously mentioned study by Dunford et al. followed the same methodology as the current study while storing the bovine tissue in DMEM. The resulting average failure stresses were 37.3±15.1kPa, 40.4±12.1kPa, and 36.0±11.3kPa at the 6hr, 24hr, and 48hr time points, respectively. The average failure strains were 0.24±0.044, 0.22±0.026, and 0.25±0.041, at the 6hr, 24hr, and 48hr time points, respectively.

To assess the effect of preservation fluid type on the tensile failure properties of liver parenchyma, the results of the current saline tests were compared to the previously published DMEM tests (Figures 6 and 7) (Dunford, 2017). The plots of average failure stress showed no significant change with respect to time for either study. Conversely, the failure strain for the tissue stored in saline decreased significantly with increased postmortem time, while no significant change in failure strain was observed for the tissue stored in DMEM. It was anticipated that DMEM would preserve the cellular architecture and material properties more effectively than the saline. In a preliminary histology study, Kemper et al. evaluated the effects of storing bovine liver tissue in DMEM for 24 hours at a cellular level (Kemper, 2013). The histological analysis showed that the DMEM maintained specimen hydration, preserved the cellular architecture, and allowed only mild cell swelling of the parenchyma (i.e., no cell dissociation or nuclear dissolution). This finding was in contrast to a histological analysis performed by Popovic et al. in which liver tissue was stored in saline (Popovic, 1989). Popovic et al. observed severe cellular swelling in guinea pig livers within two hours postmortem when the tissue was stored in saline. At four hours postmortem, Popovic et al. observed regions of complete destruction of nuclear and cellular membranes. When the results of the current study are considered in conjunction with previous histological and material property studies, it is clear that DMEM preserves the cellular structure and material properties of liver parenchyma more effectively than saline within the first 48hrs postmortem. In addition, the changes in the failure properties with increased postmortem time observed in the liver tissue stored in saline appear to be related to changes in the cellular structure. Future work will aim to assess any changes at the cellular level with respect to postmortem time through a histological study performed on tissue samples obtained from the livers used in the current study and the previous study performed by Dunford et al. (2017).

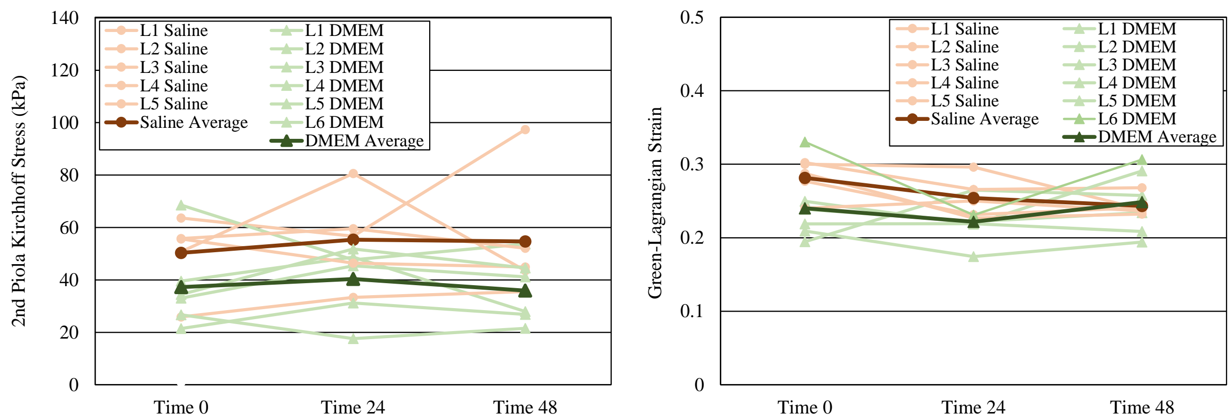

Figure 6. Comparison of Average Failure Stress (left) and Average Failure Strain (right) for Tissue Stored in DMEM (Dunford, 2017) and Saline at each Time Point.

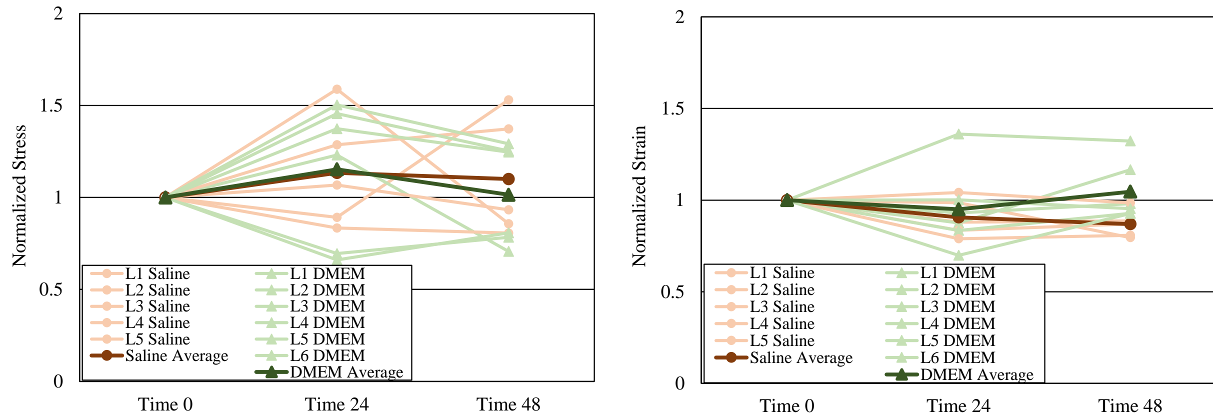

Figure 7. Comparison of Normalized Average Failure Stress (left) and Average Failure Strain (right) for Tissue Stored in DMEM (Dunford, 2017) and Saline at each Time Point.

CONCLUSIONS

This study conducted uniaxial tension tests on bovine liver samples to quantify the effects of postmortem time on the tensile failure properties when the tissue was stored in saline. A total of 51 dog-bone specimens from five bovine livers were successfully tested across three time points. Liver tissue was stored in normal saline and kept cool between the 6hr, 24hr, and 48hr time points. The average failure 2nd Piola Kirchhoff stress and Green-Lagrangian strain were calculated for each liver at each of the three time points. There were no significant changes in failure stress with respect to postmortem time. However, there was a significant decrease in failure strain with increased postmortem time. The results from the current study and a previous study, which stored liver tissue in DMEM, were compared to show that the effects of postmortem degradation vary with the preservation fluid used. Specifically, DMEM was found to preserve the material properties of liver parenchyma more effectively than saline within the first 48hrs postmortem.

REFERENCES

DUCKWORTH, M. P., IEZZI, A., IEZZI, T., & O'DONOHUE, W. T. (2008). Motor Vehicle Collisions: Medical, Psychosocial, and Legal Consequences (1st ed.). Academic Press.

KEMPER, A.R., SANTAGO, A.C., STITZEL, J.D., SPARKS, J.L., DUMA, S.M. (2010). Biomechanical response of human liver in tensile loading. Ann. Adv. Automot. Med., vol. 54, 15-26,

KEMPER, A.R., SANTAGO, A.C., STITZEL, J.D., SPARKS, J.L., DUMA, S.M. (2013). Effect of Strain Rate on the Material Properties of Human Liver Parenchyma in Unconfined Compression. J of Biomech Eng, vol. 135(10).

KLINICH, K. D., FLANNAGAN, C. A. C., NICHOLSON, K., SCHNEIDER, L. W., RUPP, J. D. (2010). Factors associated with abdominal injury in frontal, farside, and nearside crashes. Stapp car crash journal, 54, 73-91.

MALAKI, M., MANGAT, K. (2011). Hepatic and splenic trauma. Trauma, 13(3), 233-244.

OTTENSMEYER, M.P. (2001). "Minimally invasive instrument for in vivo measurement of solid organ mechanical impedance," Ph.D. dissertation, Dept. Mech. Eng., Massachusetts Inst. of Technol.

PERICHON, N., OUDRY, J., CHATELIN, S., SANDRIN, L., ALLEMANN, P., SOLER, L., WILLINGER, R. (2009). In vivo liver tissue mechanical properties by transient elastography: comparison with dynamic mechanical analysis. IRCOBI Conference. 57-68.

POPOVIC, D., SIMIC, M. (1989). The early post mortem histological changes under experimental conditions. Acta medicinae legalis et socialis, vol. 39, 219-226.

SANTAGO, A.C., KEMPER, A.R., MCNALLY, C., SPARKS, J.L., DUMA, S.M. (2009). The effect of temperature on the mechanical properties of bovine liver. Biomedical Sciences Instrumentation, vol. 45, 376-381.

SANTAGO, A.C., KEMPER, A.R., MCNALLY, C., SPARKS, J.L., DUMA, S.M. (2009). Freezing affects the mechanical properties of bovine liver. Biomedical Sciences Instrumentation, vol. 45, 24-29.

STINGL, J., BACA, V., CECH, P., KOVANDA, J., KOVANDOVA, H., MANDYS, V., REJMONTOVA, J., SOSNA, B. (2002). Morphology and some biomechanical properties of human liver and spleen. Surgical and Radiologic Anatomy, 24(5), 285-289.

TAY, B., Kim, J., SRINIVASAN, M. (2006). In vivo mechanical behavior of intra-abdominal organs. IEEE Trans. on Biomedical Engineering, vol. 53(11), 2129-2138.

TOMITA, Y., NIHIRA, M., OHNO, Y., SATO, S. (2004). Ultrastructural changes during in situ early postmortem autolysis in kidney, pancreas, liver, heart and skeletal muscle of rats. Legal Medicine, vol. 6, 25-31.

UEHARA, H. (1995). Study on the Mechanical Properties of the Kidney, Liver, and Spleen, by Means of Tensile Stress Test with Variable Strain Velocity. Journal of Kyoto Prefectural University of Medicine., 104(1), 439-451.